Solid State Communications, Vol 65, No 7, pp 693–696, 1988
Printed in Great Britain

0038–1098/88 $3 00 + 00
Pergamon Journals Ltd

NUCLEAR SPIN–LATTICE RELAXATION AND EFFECTS OF SHORT-RANGE ORDER IN Cu_x–Pt_{1-x}

J Banhart, H Ebert and J Voitlander

Institut fur Physikalische Chemie, Universitat Munchen Sophienstrasse 11, 8000 Munchen 2, FRG

and

P Weinberger

Institut fur Technische Elektrochemie, Technische Universitat Wien Getreidemarkt 9, 1060 Wien, Austria

(*Received* 3 *September* 1987 *by P H Dederichs*)

Densities of states and nuclear spin-lattice relaxation rates are calculated for Cu_x–Pt_{1-x} Effects of short-range order are included in terms of the fully relativistic Embedded Cluster Method Specific heats are calculated and compared with experimental results

1 INTRODUCTION

SINCE IN SUBSTITUTIONAL alloys nuclear spin–lattice relaxation rates map neighbourhood dependent partial local densities of states at the Fermi energy, these rates offer the possibility to discuss effects of short-range order and segregation in a compact form The rates can be calculated as a function of the neighbourhood configuration and can be displayed vs the number of atoms of one component occupying a particular shell of neighbours or vs the short-range order parameters, respectively A comparison with the corresponding results for the statistically disordered case allows a quantitative illustration for the validity of the Coherent Potential Approximation (CPA) A comparison with experimental values can be used to interpret data corresponding to one and the same "macroscopical" concentration, however, obtained from samples of different preparational origin and therefore different stages of order In the present Communication the theoretical Pt nuclear spin–lattice relaxation rates in Cu_x–Pt_{1-x} are discussed for a series of concentrations considering all possible configurations of a first shell of neighbours cluster and are compared with available experimental data For $Cu_{50}Pt_{50}$ short-range order effects resulting from a shell of second neighbours are also taken into account In addition experimental order-dependent specific heats are interpreted All calculations are performed using the fully relativistic Embedded Cluster Method (ECM) [1] and are based on results obtained within the frame-work of the fully relativistic KKR-CPA method [2] In the following section the applied methods are very briefly recalled

2 THEORETICAL ASPECTS

For cubic lattices with only one atom per unit cell the off-diagonal scattering-path operator for substitutional alloys is defined as follows [1]

$$\begin{aligned}\tau(\boldsymbol{R}_i - \boldsymbol{R}_j) = \tau^{ij} &= (1/\Omega_{BZ}) \\ &\times \int_{BZ} [\mathbf{t}_c^{-1} - \mathbf{G}(\boldsymbol{k})]^{-1} \\ &\times \exp[i\boldsymbol{k}\,(\boldsymbol{R}_i - \boldsymbol{R}_j)]\mathrm{d}^3k \\ &= (2/\Omega_{IBZ}) \sum_{S\in 0} \int_{IBZ} \\ &\times \mathbf{D}(S)^{\dagger}\tau(\boldsymbol{k})\mathbf{D}(S) \\ &\times \cos[\mathbf{S}\boldsymbol{k}\,(\boldsymbol{R}_i - \boldsymbol{R}_j)]\mathrm{d}^3k \qquad (1)\end{aligned}$$

$\mathbf{t}_c$ is the effective single site t-matrix [2] and $\mathbf{G}(\boldsymbol{k})$ are the KKR structure constants The matrices $\mathbf{D}(S)$ contain blockwise the Clebsch–Gordan coefficients for the irreducible projective representations of $0 \in 0_h$, the matrices $\{\mathbf{S}\}$ are the Γ_{15} (t_{1u})-like vector representatives of 0_h [3] Ω_{BZ} is the volume of the Brillouin zone, Ω_{IBZ} of its irreducible wedge Only a very restricted number of off-diagonal scattering path operators has to be calculated [3], namely 4 for the first shell and 2 for the second shell using the relation

$$\tau^{kl} = \mathbf{D}(S)^{\dagger}t^{ij}\mathbf{D}(S), \qquad (2)$$

with

$$|\mathbf{S}(\boldsymbol{R}_i - \boldsymbol{R}_j)| = |\boldsymbol{R}_k - \boldsymbol{R}_l|$$

In terms of the τ^{ij} the density-of-states corresponding to a particular site i occupied by species α and cluster

Table 1 Shell occupation of an equiatomic CuPt lattice (Pt-atom at the center)

Shell	Atoms	Distance from center	Disordered		Ordered	
			Cu	Pt	Cu	Pt
0	1	0	0	1	0	1
1	12	$\sqrt{2}/2$	6	6	6	6
2	6	1	3	3	6	0
3	24	$\sqrt{6}/2$	12	12	12	12
4	12	$\sqrt{2}$	6	6	0	12

configuration J can be obtained from the expression

$$n_i^\alpha(E) = -\frac{1}{\pi}\,\mathrm{Im\ tr}\,\mathbf{R}^\alpha[\tau^J]_{ii}, \tag{3}$$

where the supermatrix τ^J is defined by its elements

$$[\tau^J]_{ij} = \{(\mathbf{t}_{\alpha(i)}^{-1} - \mathbf{t}_c^{-1})\delta_{ij} + [\tau^{-1}]_{ij}\}^{-1} \tag{4}$$

The size of the supermatrix is $N\ 2\ (l_{\max} + 1)^2$, where N is the number of atoms in the cluster and $l_{\max}$ is the maximum angular momentum In equation (4) $\mathbf{t}_\alpha$ is the single site t-matrix of species α and in equation (3) R^α is a matrix of radial integrals [4] over the Wigner–Seitz cell

$$R_{QQ'}^\alpha = \int Z_Q^\alpha(\boldsymbol{r})\, Z_{Q'}^\alpha(\boldsymbol{r})\, \mathrm{d}^3r, \quad Q = (\kappa, \mu) \tag{5}$$

Restricting the integration in equation (5) to the muffin-tin sphere, partial local densities of states for species α positioned at the center of origin ($i = 0$), corresponding to a particular configuration J, can be calculated

$$n_{\mathrm{MT}}^{J,\alpha}(E) = \sum_\kappa n_\kappa^{J\,\alpha}(E) \tag{6}$$

In equation (6) $n_{\mathrm{MT}}^{J,\alpha}(E)$ is the corresponding muffin-tin density-of-states The configuration dependent densities of states can now be used to calculate configuration dependent nuclear spin–lattice relaxations rates [5]

$$\begin{aligned}(T_1T)_{J\alpha}^{-1} = {} & 4\pi k_B\hbar\left(\gamma_N\frac{e}{2}\right)^2\left[\sum_\kappa\frac{2j+1}{6j(j+1)}\right. \\ & \times [n_\kappa^{J,\alpha}(E_F)\bar{R}_{\kappa\kappa}^\alpha(E_F)]^2 + \sum_{\kappa>0}\frac{1}{3j+1} \\ & \times n_\kappa^{J,\alpha}(E_F)n_{-\kappa-1}^{J,\alpha}(E_F) \\ & \left.\times [\bar{R}_{\kappa,-\kappa-1}^\alpha(E_F)]^2\right],\end{aligned} \tag{7}$$

where the $\bar{R}_{\kappa\kappa'}(E)$ are renormalized radial integrals In the present paper all BZ-integrals including the ones in the KKR-CPA calculations are calculated using the 21 directions of Fehlner and Vosko [6] The KKR-CPA calculations are based on potentials obtained by a Mattheiss construction using Slater exchange only

3 RESULTS

As the number of atoms of a particular species in the first shell varies from 0 to 12 for a f c c lattice a total of 144 configurations has to be calculated Going beyond a first shell of neighbours, the number of configurations increases dramatically For $Cu_{50}Pt_{50}$ however, it was argued that in accordance with the CuPt structure (Table 1) short-range ordering seems to occur not in the first shell, but in the second shell or beyond This particular case can easily be handled in the present approach, because by putting "effective" (CPA) atoms to the positions of the first shell only 10 different second shell configurations have to be considered Including the second shell, however, implies that the size of the matrix in equation (4) increases from 234 for one shell only to 342

In Figs 1(a) and 1(b) the variation of the density-of-states (equation 3) in $Cu_{50}Pt_{50}$ at the Fermi energy is shown with respect to the number of Cu(Pt) atoms in the first shell Each cross represents one configuration Since in this particular alloy the Fermi energy falls into the edge of the Pt-d-band, the variation with respect to the different occupations is considerably large In Fig 1(c), showing the effects of short-range ordering with respect to the second shell, the variation of the Pt density-of-states is only slightly smaller than in Fig 1(b) It should be noted that Fig 1 serves as a beautiful illustration for the fact that the CPA indeed represents a configurational average

Turning now to the Pt nuclear spin–lattice relaxation rates shown in Fig 2, one can see that in $Cu_{50}Pt_{50}$ effects due to local arrangement are quite pronounced these effects are large for both cases, namely for the first shell cluster (Fig 2a) and the second shell cluster (Fig 2b) In $Cu_{71}Pt_{29}$ effects due to local arrangement are much less drastic than in $Cu_{50}Pt_{50}$ This of course has to be expected since in $Cu_{71}Pt_{29}$ the Fermi energy

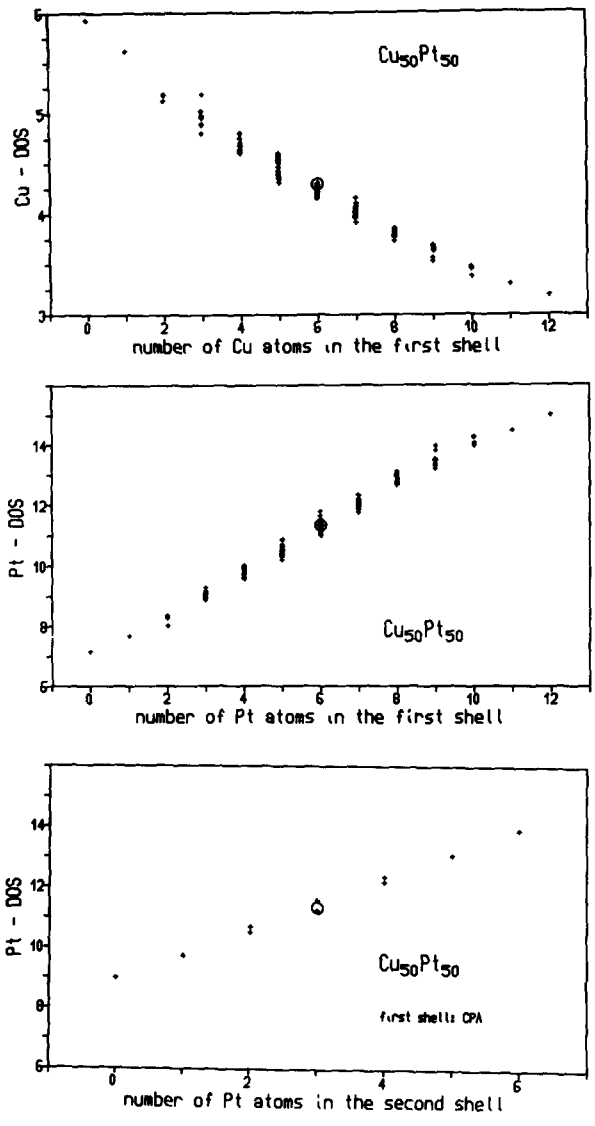

Fig 1. (a) Density-of-states at E_F in a first neighbour cluster in $Cu_{50}Pt_{50}$ with Cu at the center (b) Density-of-states at E_F in a first neighbour cluster in $Cu_{50}Pt_{50}$ with Pt at the center (c) Density-of-states at E_F in a second neighbour cluster in which the first shell consists of CPA atoms (statistical disorder) and Pt is at the center In a–c the crosses correspond to the possible configurations, the circles to the KKR-CPA results Densities of states are given in (states/ry atom)

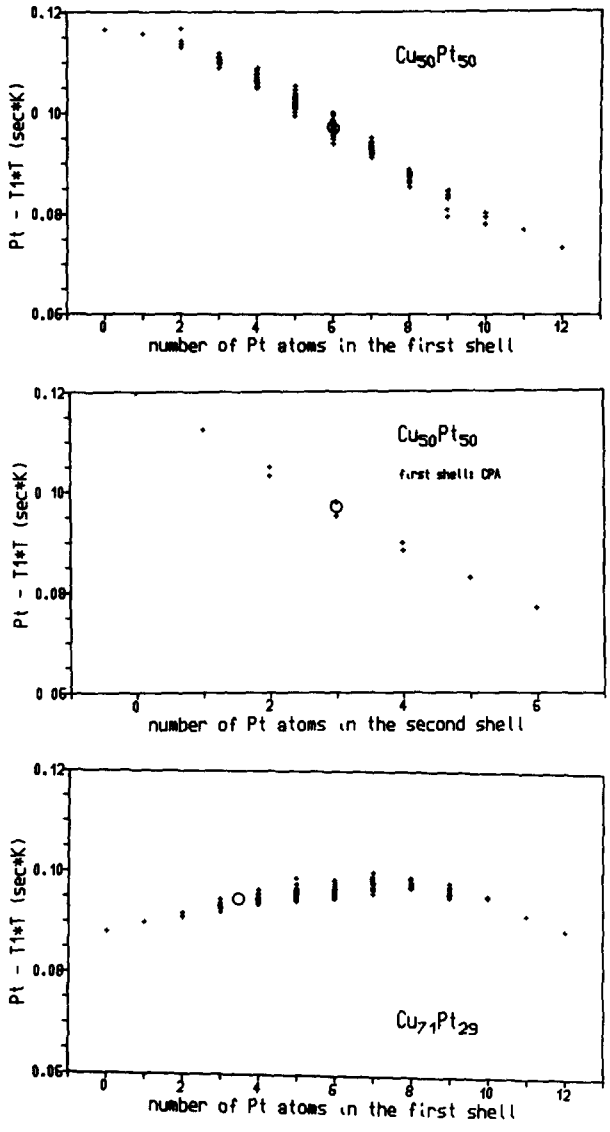

Fig 2 (a) Pt-nuclear spin–lattice relaxation rates in $Cu_{50}Pt_{50}$ with the occupation in the first shell varied (b) Pt-nuclear spin–lattice relaxation rates in $Cu_{50}Pt_{50}$ with the occupations in the second neighbour shell varied and CPA atoms in the first shell (c) same as (a) in $Cu_{71}Pt_{29}$ In a–c the crosses correspond to the possible configurations, the circles to the KKR-CPA results Note that for matters of convenience the inverse of the relaxation rate (1/(sec k)) is shown

falls into the onset of the s-band above the d-band It should be noted from Figs 1 and 2 that values to the right of the CPA value are due to "like-wise" ordering (segregation), whereas the values to the left incorporate the cases with "anti-like-wise" ordering (short-range order) In terms of the Warren-Cowley SRO-parameters α_r, which are defined for an A atom at the center as

$$\alpha_r = 1 - n_r/(c_B n_r^B), \tag{7}$$

(n_r is the number of all atoms in the r-th shell, n_r^B that of B atoms) values to the right of the CPA value in Figs 1 and 2 correspond to positive α_r and vice versa Figure 3 finally summarizes the obtained results with

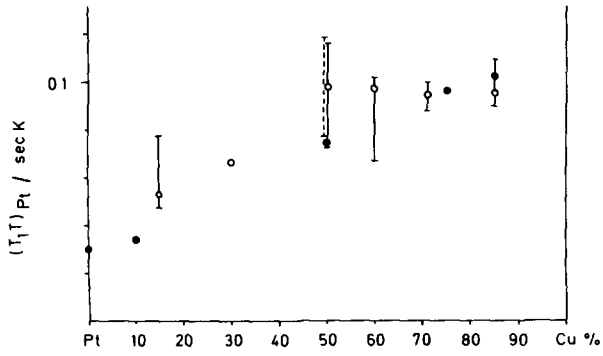

Fig 3 Pt-nuclear spin–lattice relaxation rate in Cu_xPt_{1-x} full circles experimental data [7], open circles KKR-CPA results, full bars range of variation with respect to first neighbour shell configurations, dashed bar range of variation with respect to second neighbour shell configurations and CPA atoms occupying the first shell

respect to the "macroscopical" concentration and compares them with the experimental values [7] This figure indicates that for Cu-rich Cu_xPt_{1-x} alloys such as $Cu_{71}Pt_{29}$ local arrangement effects are of minor importance whereas for Pt-rich alloys these effects gain importance By comparing the theoretical values with the experimental data [7], it is seen from Fig 3 that for Cu-rich or Pt-rich Cu_xPt_{1-x} alloys the agreement indeed is excellent Unfortunately in [7] no account is given of how the samples were prepared It is therefore difficult to comment on the fact that for $Cu_{50}Pt_{50}$ the experimental value is considerably below the CPA value, i e in the regime of segregation

By approximating the DOS for the long-range ordered state in $Cu_{50}Pt_{50}$ by a two shell cluster corresponding to the occupations in the CuPt structure, one effectively includes also a third shell, since this third shell contains in the ordered structure 6 atoms of each kind (Table 1), a situation which is well represented by the embedding CPA medium Together with the DOS for the statistically disordered case (CPA) this approximated DOS for the ordered case, can be compared with experimental γ values of the linear coefficient of the specific heat [8] According to [9] however, the values of [8] contain an arithmetic error and have to be multiplied by a factor of 1 93 The coefficient γ is predicted by the calculations to change from 1 34 to 1 08 mJ K mol^{-1} due to ordering This result is in nice agreement with the experimental findings for disordered (1 59 mJ K mol^{-1}) [9] and ordered (1 03 mJ K mol^{-1}) [8, 9] $Cu_{50}Pt_{50}$

Acknowledgements — One of us (JB) wants to acknowledge financial support by the Deutsche Forschungsgemeinschaft (DFG)

REFERENCES

1 P Weinberger, R Dirl, A M Boring, A Gonis & A J Freeman, *Phys Rev B*, submitted for publication
2 J Staunton, B L Gyorffy & P Weinberger, *J Phys F Metal Phys* **10,** 2665 (1980)
3 R Dirl, R Haase, P Herzig, P Weinberger & S L Altmann, *Phys Rev* **B32,** 788 (1985)
4 P Weinberger, J Staunton & B.L Gyorffy, *J Phys F Metal Phys* **12,** 2229 (1982)
5 H Ebert, P Weinberger & J Voitlander, *Phys Rev* **B31,** 7566 (1985)
6 W H Fehlner & S H Vosko, *Can J Phys* **54,** 2159 (1976)
7 J Itoh, K Asayama & S Kobayashi, *Proc Coll Ampere* **13,** 162 (1964)
8 B Roessler & J A Rayne, *Phys Rev* **136,** A1380 (1964)
9 D L Martin, *Phys Rev* **B17,** 1674 (1978)